RESEARCH ARTICLE

Two-Step Approach for Improving the Distribution Network Voltage Profile Using the Optimal Integration of the PV-BES System

Nikola Krstić[1,*] **and Dragan Tasić**[1]

[1] Faculty of Electronic Engineering, University of Niš, 18104 Niš, Serbia

Abstract

This paper proposes the two-step approach for improving the voltage profile of the distribution network (DN) using the optimal integration of photovoltaic-battery energy storage (PV-BES) system. In the first step of the approach the optimal location of the PV-BES system in the DN and its optimal powers are determined, considering the topology and the load of the DN. This is done to improve the voltage profile of the DN using the meta-heuristic wild horse optimization method (WHO) and genetic algorithm (GA). The second step of the approach determines the optimal sizing of the PV-BES system, by taking into account the optimal powers obtained in the first step, the solar irradiance diagram and the average temperature for each month of the year for the area in which the DN is located. The optimal sizing includes optimal maximum power of the PV system and the optimal maximum power and energy capacity of the BES unit, determined by the proposed iterative method. The results are generated using the topology of the IEEE 18-bus radial DN for three different load diagrams, on a monthly and annual basis.

Keywords: distribution network (DN), genetic algorithm (GA), photovoltaic-battery energy storage (PV-BES) system, voltage profile, wild horse optimization (WHO).

1 Introduction

One of the key aspects of the quality of the distribution network (DN) operation is its voltage profile [1]. To improve the voltage profile of the DN adequate power flows in the network branches must be achieved. This can be done by connecting the distributed generation [2] in the DN, whose power unlike the load can be controlled. In this paper the photovoltaic-battery storage (PV-BES) system is used as a controlled distributed generation [3, 4], considering that energy produced by the PV system can be properly injected into the DN during the whole observation period using the BES unit [5]. In other words, the BES unit is used to provide the injection of the optimal power, produced by the PV system, into the DN by charging or discharging itself in the time of high or low solar irradiance, respectively [6].

To efficiently implement the idea mentioned above, a two-step approach is proposed in this paper. In the first step of the approach the optimal powers needed to improve the voltage profile of the DN and the optimal

Submitted: 26 February 2026
Accepted: 19 March 2026
Published: 22 March 2026

Vol. 2, **No.** 1, 2026.
10.62762/TEPNS.2026.581037

***Corresponding author:**
✉ Nikola Krstić
nikola.krstic@elfak.ni.ac.rs

Citation
Krstić, N., & Tasić, D. (2026). Two-Step Approach for Improving the Distribution Network Voltage Profile Using the Optimal Integration of the PV-BES System. *ICCK Transactions on Electric Power Networks and Systems*, 2(1), 31–46.

location of their injection are determined [7, 8], using the meta-heuristic optimization methods of genetic algorithm (GA) [9, 10] and wild horse optimization (WHO) [11, 12]. This is done considering the load diagram and the topology of the DN, where the voltage quality index of the DN is used as a criterion function. In addition to the first step which represents the well-known procedure, based on meta-heuristic optimization methods [13–15], for improving the voltage profile of the DN using distributed generation, the second step of the proposed approach contains elements that can be regarded as novel and represents the main contribution of the paper.

Second step of the approach refers to the optimal sizing of the PV-BES system [16, 17] in which the necessary maximum power of the PV system, and the necessary maximum power and the energy capacity of the BES unit are determined [18–20]. This is achieved using the proposed iterative method, which represents a unique procedure for sizing the PV-BES system [21] by adjusting the necessary maximum power of the PV system [22–24] through iterations to achieve the optimal powers of the PV-BES system, while maintaining the desired state of charge of the BES unit. Input information for the iterative method are the optimal powers of the PV-BES system obtained in the first step and the power generation diagram of the PV system for each month of the year, expressed per unit. The procedure for determining the power generation diagram of the PV system per unit combines the influence of solar irradiance and temperature on the PV system power generation [25, 26] using the analogy between the solar irradiance and the power of the PV panels [25] to maximize their energy production. The mentioned procedure is the quick and simple technique to determine the shape of the power generation diagram of the PV system which maximizes the energy production [27] and operates without partial shading, representing the additional contribution of the paper. It is assumed that the PV system consists of fixed PV panels, so the maximization of its energy production is achieved using the optimal value of the tilt angle [28] determined within the procedure for creating the PV system power generation diagram. To determine the diffuse and the reflected component of solar irradiance on the tilted surface the isotropic cylindrical model is used [29]. The data necessary for determining the optimal tilt angle of the PV panels in the PV system and creating the PV system power generation diagram per unit is taken from the Photovoltaic Geographical Information System (PVGIS) web site using the PVGIS-SARAH3 database. These data includes the values of total and diffuse component of solar irradiance on the horizontal surface and the average temperature values for each month in the year, for the area of the DN.

To see the impact of higher or lower matching level between the solar irradiance and the load, three different load diagrams of the DN are used for generating results [30]. All results are generated using the topology of IEEE 18-bus radial DN, considering the cases of different efficiencies of the BES unit. Also, to measure the influence of the solar irradiance diagram on the optimal sizing of the PV-BES system, different operating periods are considered including each month in the year and the year in total, which is rarely the case in the similar literature.

2 Optimal Powers and Location of the PV-BES System

The optimal powers and location of the PV-BES system are generated using the meta-heuristic optimization methods of GA and WHO, as a solution to the optimization problem of improving the voltage profile of the DN. The meta-heuristic optimization methods are used because they are widespread in scientific literature and prove to be very efficient for optimizing the different aspects of the DN operation. Specifically, the authors chose the GA because in addition to the particle swarm optimization (PSO), is one of the fundamental meta-heuristic optimization algorithms, and the WHO is chosen as relatively new meta-heuristics which combines the elements from GA and PSO.

2.1 Genetic Algorithm

The GA is the population based meta-heuristic optimization method, inspired by the process of natural selection in the evolution theory [31]. It mimics the process in which more suitable and adaptable individuals have better chance to survive and produce the offspring. Each individual in the population is described with the vector of control variables, and its genes are coordinates of that vector. As the genes determine the suitability of the individual in nature, vector of control variables determines the criterion function of the individual which quantifies its fitness.

One iteration of this optimization method consists of three major steps, including selection, crossing and mutation [9, 10]. In the selection process, individuals are selected for mating from the population genetic pool, where the more fitted individuals have greater

probability to be selected. Specifically, in this paper the elitist approach is used in which only the certain percent of fittest individuals can be chosen for mating [13]. The probability P of the i-th fittest individual to be chosen from the genetic pool is determined using the expression:

$$P(i) = \frac{N - i + 1}{\sum_{i=1}^{N} i}, \tag{1}$$

The crossing of the genes of the chosen individuals takes place in the second step, where the new individual is created [13]. Specifically, in this paper the gen for the location of PV-BES system is inherited from one of the parents, while the genes for the powers of the PV-BES system are determined using the arithmetic crossing [21].

$$loc_0 = loc_1, \tag{2}$$

$$P_{\text{PV-BES}j0} = (P_{\text{PV-BES}j1} + P_{\text{PV-BES}j2})/2, \tag{3}$$

where loc_0 and loc_1 are the locations of the PV-BES system of the offspring and one of the parents, respectively, while $P_{\text{PV-BES}j0}, P_{\text{PV-BES}j1}$ and $P_{\text{PV-BES}j2}$ are the powers of the PV-BES system in the j-th hour of the offspring, first and second parent, respectively.

Mutation as the third step of the GA [13], emulates the random change of the genes that happen in nature, by randomly changing the values of the individuals control vector coordinates, with certain probability.

$$\begin{aligned} loc_i &= loc_i - 1, \quad r < p_i, \\ loc_i &= loc_i + 1, \quad r > 1 - p_i, \end{aligned} \tag{4}$$

$$P_{\text{PV-BES}j,i} = P_{\text{PV-BES}j,i} + (2r - 1)\Delta P_{\text{PV-BES}}, \tag{5}$$

where loc_i is the location, and $P_{\text{PV-BES}j,i}$ is the power of the PV-BES system in the j-th hour of the i-th individual, $\Delta P_{\text{PV-BES}}$ is the maximum change of the PV-BES power, r is the random value from the interval $[0, 1]$ and p_i is the preset probability. Considering this, the mutation represents the mechanism of GA for escaping the local optimum. Repeating the mentioned steps through the iterations the optimization method finds the optimal solution of the optimization problem.

2.2 Wild Horse Optimization

The WHO represents the population based meta-heuristic optimization method, inspired by the life of the wild horses in nature. Considering this, the four major steps of the WHO are based on the four characteristic behaviors of the wild horses in nature, including grazing, mating, group leadership and selection of the group leader [32]. Before these four steps that are repeated through the iterations, there is the initial step of group creation. In the initial step the population of wild horses is separated into the groups with equal number of individuals, and one stallion. The stallion is the individual with the best value of the criterion function.

In the grazing field the individuals move within the circle [32], in the center of which is the stallion, and it can be analytically expressed as:

$$\vec{H'}_{j,p} = A\cos(r\pi)(\vec{S}_p - \vec{H}_{j,p}) + \vec{S}_p, \tag{6}$$

where $\vec{H'}_{j,p}$ and $\vec{H}_{j,p}$ are the vectors of control variables of the j-th individual in the group p, after and before grazing, $\vec{S}_p$ is the vector of control variables of the stallion in the group p, r is the random value from the interval $[0, 1]$, while A is the radius of the circle, which changes its value through the iterations as:

$$A = A_{\max} - \frac{it}{N_{it}}(A_{\max} - A_{\min}), \tag{7}$$

where it and N_{it} are the ordinal and total number of iterations, respectively.

The second step in the WHO is the mating process in which the crossing of genes of the parents takes place, creating the new individual [11, 12]. This step appears with certain probability and for it the arithmetic crossing is used as in GA, analytically expressed with (2) and (3). It is important to emphasize that mare and stallion which are mating must not be from the same group. Also, with a certain probability, the newborn individual can leave its mother and join the other group.

In the third step of the optimization method the process of group leadership is described [11, 12], where the stallion leads the group to the waterhole, while competing with the stallions from other groups for the better place. The movement of the stallion is described using the following expression:

$$\vec{S'}_p = A\cos(r\pi)(\overrightarrow{WH} - \vec{S}_p) + \overrightarrow{WH}, \tag{8}$$

where $\vec{S'}_p$ and $\vec{S}_p$ are the vectors of control variables of the stallion after and before the group leadership,

while $\overrightarrow{WH}$ is the vector of control variables of the waterhole. It is important to emphasize that waterhole is located in the place with the best criterion function found so far.

The fourth and the final step of the WHO is the selection of the group leader. Namely, considering the change of the position of the stallion and the individuals in the group in the previous steps, the group leader role (stallion) must be determined again. This is done by comparing the values of the criterion function of the individuals in each group, including the stallions. The individuals with the best criterion functions in the groups are declared as the group leaders.

The optimization method generates the solution of the optimization problem by repeating the mentioned four steps sufficient number of times.

2.3 Defining and Solving the Optimization Problem

Optimization problem of determining the optimal location and powers of the PV-BES system to maximize the improvement of the voltage profile of the DN is the nonlinear optimization problem with constraints [33]. Control variables in this optimization problem are the average hourly powers and the location of the PV-BES system, which constraints are:

$$loc_{\text{PV-BES}} = \{i_1, i_2, \ldots, i_n\}, \tag{9}$$

$$P_{\text{PV-BES}}(h) < P_{\max}, \tag{10}$$

where the location of the PV-BES system $loc_{\text{PV-BES}}$ can be one of the DN nodes with indexes $\{i_1, i_2, \ldots, i_n\}$, while the power of the PV-BES system in the h-th hour $P_{\text{PV-BES}}(h)$ must be lower than the maximum power $P_{\max}$ which is allowed to be injected in this type of DN.

On the other hand, the dependent variables in the optimization problem are voltages in the DN nodes and the currents in the DN branches, which values change due to the PV-BES system power injection [16]. Constraints of the dependent variables are defined considering the allowed limits for voltage and currents in the DN, given by the expressions:

$$U_{\min} < U_i < U_{\max}, \tag{11}$$

$$I_j < I_{j\,\max}, \tag{12}$$

where voltage of the i-th node must be between minimum $U_{\min}$ and maximum $U_{\max}$ allowed values, defined by the voltage level of the DN, while current in the j-th branch I_j must be lower than the maximum allowed current in the j-th branch $I_{j\,\max}$, defined by the cross section of its conductors.

Quality of the voltage profile of the DN is quantified using the voltage quality index VQI [8], defined as the sum of the squared deviations of the voltage in relation to the reference value:

$$VQI = \frac{1}{N_h} \sum_{h=1}^{N_h} \left(U_i(h) - U_{\text{ref}}\right)^2, \tag{13}$$

where $U_i(h)$ is the voltage of the i-th node in the h-th hour, U_{ref} is the reference voltage, while N_h is the number of nodes in the DN and N_h number of hours in the observation period. Considering that the goal of optimization is to maximize the improvement of the DN voltage profile [7], the one-parameter criterion function CF equal to the voltage quality index is used:

$$CF = VQI, \tag{14}$$

To keep the voltage in the DN nodes and the current in the DN branches in the allowed range given by (11) and (12), the criterion function of the individuals whose voltage and currents are out of limits is multiplied with 100. This ensures that such individuals have practically no effect on the individuals generated for the next iteration of the optimization process and have no chance to be the solution of the optimization problem. To achieve this the voltage and current vectors of each individual, obtained after the power flow calculation, are compared with the allowed limits.

To solve the optimization problem, the criterion function is (14) minimized using the mentioned optimization methods of GA and WHO. The initial values of the individuals in the population are randomly generated, considering (9) and (10). Individuals in the population are described with the vector of control variables, that has 25 coordinates, where the first coordinate is reserved for location and other 24 are used for average hourly powers of the PV-BES system. Values of these coordinates are changing by the optimization method algorithm. After sufficient number of iterations, when the change of the criterion function is negligible, the solution to the optimization problem is determined as the vector of control variables of the individual with the best (minimal) value of the criterion function found in all iterations.

3 Determining the Power Generation Diagram of the PV System

Power generation diagram of the PV system expressed per unit is determined using the assumption that there is no partial shading on the surface of the PV panels. This means that the power generated by the PV system is proportional to the solar irradiance on the surface of its panels [25]. The influence of the PV panels temperature variation during the year on their power production, is included using the temperature coefficient of power reduction of the PV panels [26].

3.1 Determining the Solar Irradiance on the Surface of the PV Panels

Solar irradiance on the surface of the PV panels is determined considering the tilt angle of the PV panels and the data of the total and diffuse component of the solar irradiance on the horizontal surface taken from the PVGIS-SARAH3 database. For maximizing the power generation of the PV system, it is assumed that the PV panels are oriented to the south, with zero azimuth angle [27]. Taking into account that solar irradiance consists of three components, the total solar irradiance on the PV panel surface G_C with the tilt angle Σ is:

$$G_C = G_{BC} + G_{DC} + G_{RC}, \tag{15}$$

where G_{BC} is direct, G_{DC} diffuse and G_{RC} reflected component of solar irradiance on the PV panel surface, tilted by the angle Σ [34]. The direct component of the solar irradiance on the PV panel surface is determined as:

$$G_{BC} = G_{BH} R_B, \tag{16}$$

where G_{BH} is the direct component of solar irradiance on the horizontal surface, determined using the measured values of total G_H and diffuse G_{DH} component of solar irradiance on the horizontal surface, as:

$$G_{BH} = G_H - G_{DH}, \tag{17}$$

while R_B is the slope factor of the PV panels surface, which is obtained using the expression:

$$R_B = \frac{\cos\theta}{\sin\beta}, \tag{18}$$

In (18) θ is the incidence angle of the direct component of the solar irradiance on the PV panel surface, and β is the altitude angle of the sun [24]. Considering that the available data for the solar irradiance is average hourly data, the mentioned angles also have average hourly values.

The diffuse and reflected components of solar irradiance on the PV panel surface are obtained using the isotropic cylindrical model [29]. This model assumes that the diffuse component comes equally from all directions from the sky, and that the reflected component of solar irradiance comes equally from all directions from the ground, in a cylindrical coordinate system [24]. Considering that tilting the PV panel surface disables the diffuse radiation from certain directions to arrive on it, the diffuse component of solar irradiance is reduced and can be determined as:

$$G_{DC} = G_{DH} \frac{1 + \cos\Sigma}{2}, \tag{19}$$

On the contrary the reflected component is increasing by tilting the PV panel, because in that case reflected solar radiation can arrive on the surface of the PV panel in more directions [24]. Considering this, the reflected component of solar irradiance on the PV panel surface with the tilt angle Σ and the reflection coefficient ρ is:

$$G_{RC} = \rho G_H \frac{1 - \cos\Sigma}{2}, \tag{20}$$

3.2 Influence of the Temperature on the PV System Power Generation

To determine the influence of the temperature on the PV system power generation it is necessary to calculate the temperature of the PV panel cells θ_c [26]. This temperature is determined as the sum of the ambient temperature θ_a and the temperature increment which occurs due to the solar irradiance on the PV panel surface, using the following expression:

$$\theta_c = \theta_a + \frac{NOCT - 20}{800} G_c, \tag{21}$$

where $NOCT$ is the normal operating cell temperature. It is important to notice that the solar irradiance in (21) is expressed in $[W/m^2]$ and the ambient temperature is in $[^\circ C]$. Now, the dependency of the power of the PV system on its temperature can be determined using the temperature coefficient of the PV panels power reduction k_p [26] as:

$$P_{PV}(\theta_c) = P_{PV}(25^\circ C)\big(1 - k_p(\theta_c - 25^\circ C)\big), \tag{22}$$

where $P_{PV}(\theta_c)$ and $P_{PV}(25^\circ C)$ are the powers of the PV system on the θ_c and $25^\circ C$ temperature, respectively. Using the obtained values of the solar

irradiance on the PV panel surface [25] and its temperature, the average hourly power of the PV system in the h-th hour, expressed per unit, $p_{PV}(h)$ is determined using the expression:

$$p_{PV}(h) = \frac{G_c(h)}{G_{c\max}}\big(1 - k_p(\theta_c(h) - 25°C)\big), \tag{23}$$

In (23) $\theta_c(h)$ and $G_c(h)$ are the average values of temperature and solar irradiance on the PV panel surface in the h-th hour determined by using the mentioned procedure and the available data of the average hourly values of the total and diffuse component of solar irradiance on the horizontal surface and the ambient temperature, while $G_{c\max}$ is the maximum solar irradiance on the PV panel surface in the observed period.

Power generation diagram of the PV system expressed per unit is created using (23) in which solar irradiance on the PV panel surface is calculated using the value of the tilt angle that maximizes the energy generated by the PV system [28]. Taking into account the proportionality between the solar irradiation and the energy generated by the PV system and considering the influence of the temperature on the PV system power generation, maximization of the energy generated by the PV system is achieved by maximizing the solar irradiation I_c from the following expression:

$$I_c = \sum_{h=1}^{N_h} G_c(h)\big(1 - k_p(\theta_c(h) - 25°C)\big), \tag{24}$$

4 Optimal Sizing of the PV-BES System

In this paper the optimal sizing of the PV-BES system [35] is the sizing which enables the injection of optimal powers into the DN with minimal resources [16]. The first step in the sizing of the PV-BES system is the calculation of the maximum necessary power of the PV system using the proposed iterative method.

4.1 Iterative Method for Sizing the PV System

The goal of the iterative method used for sizing the PV system is to determine its necessary maximum power needed for optimal power injection of the PV-BES system, while maintaining the state of charge of the BES unit at the end of the operation cycle SOC_T as it was at the beginning, SOC_0.

$$P_{\text{PV-BES}}(h) = P_{op}(h), \tag{25}$$

$$SOC_T - SOC_0 = 0, \tag{26}$$

where $P_{op}(h)$ is the optimal power injection in the h-th hour considering the DN voltage profile improvement. To achieve this the iterative method is adjusting the maximum power of the PV system through the iterations by better estimating the periods of charging and discharging the BES unit [16]. The assumption of the value of the maximum power of the PV system in the initial iteration of the iterative method $P^1_{PV\max}$ is calculated considering the ideal process of charging and discharging of the BES unit, using the following expression:

$$P^1_{PV\max} = \frac{\sum_{h=1}^{N_h} P_{op}(h)}{\sum_{h=1}^{N_h} p_{PV}(h)}, \tag{27}$$

Now, the charging and discharging hours of the BES unit in the k-th iteration h^k_{ch} and h^k_{dch} are determined from the (28) and (29) respectively.

$$P^k_{PV\max} \cdot p_{PV}(h) \geq P_{op}(h), \quad h^k_{ch} = h, \tag{28}$$

$$P^k_{PV\max} \cdot p_{PV}(h) < P_{op}(h), \quad h^k_{dch} = h, \tag{29}$$

Using the estimated periods of charging and discharging in the k-th iteration, maximum power of the PV system in the $k+1$-th iteration is determined as:

$$P^{k+1}_{PV\max} = \frac{\eta \sum P_{op}(h^k_{ch}) + \frac{1}{\eta}\sum P_{op}(h^k_{dch})}{\eta \sum p_{PV}(h^k_{ch}) + \frac{1}{\eta}\sum p_{PV}(h^k_{dch})}, \tag{30}$$

By repeating the steps given in (28), (29) and (30), the iterative method better estimates the value of the necessary maximum power of the PV system [16]. The iterative method ends when the maximum power of the PV system has the same value in two adjacent iterations, which also represents the result of the iterative method.

4.2 Sizing the BES Unit

Sizing the BES unit includes determining the necessary maximum power and energy capacity of the BES unit [36]. To achieve this the average hourly powers of the BES unit $P_{BES}(h)$ are determined using the obtained value of the maximum power of the PV system, as:

$$P_{BES}(h) = P_{PV\,\max} \cdot p_{PV}(h) - P_{op}(h), \tag{31}$$

Considering (28), (29) and (31) it is important to notice that the power of the BES unit has positive values in the charging hours and negative values in the discharging hours. Now, the necessary maximum power of the BES unit $P_{BES\,\max}$ [18, 19], taking into account both charging and discharging periods can be determined as:

$$P_{BES\,\max} = \max\{P_{BES}(h)\}, \quad h = 1, 2, \ldots, N_h \tag{32}$$

Using the average hourly powers of the BES unit, the energy stored in the BES unit at the end of the h-th hour $W_{BES}(h)$ is obtained as:

$$W_{BES}(h) = \sum \left(\eta P_{BES}(h_{ch}) + \frac{1}{\eta} P_{BES}(h_{dch}) \right), \tag{33}$$

$$h_{ch} \neq h_{dch} \leq h, \tag{34}$$

The necessary energy capacity of the BES unit must be able to provide the needed difference between the maximum and minimum level of the stored energies during the operation cycle, in the allowed range of the state of charge of the BES unit [20]. Considering this the energy capacity of the BES unit Q_{BES} is calculated from the expression:

$$Q_{BES} = \frac{\max\{W_{BES}(h)\} - \min\{W_{BES}(h)\}}{SOC_{\max} - SOC_{\min}}, \quad h = 1, 2, \ldots, N_h, \tag{35}$$

where $SOC_{\max}$ and $SOC_{\min}$ are the maximum and minimum allowed state of charge of the BES unit.

In Figure 1, the flowchart of the proposed two-step approach is presented.

5 Presentation and Analysis of the Results

The results are generated using a DN that has the same topology as the IEEE 18-bus radial DN, shown in Figure 2. The authors chose the IEEE 18-bus radial DN because it is less frequently used in the literature compared to the IEEE 33-bus and IEEE 69-bus DNs for this type of optimization problem, and

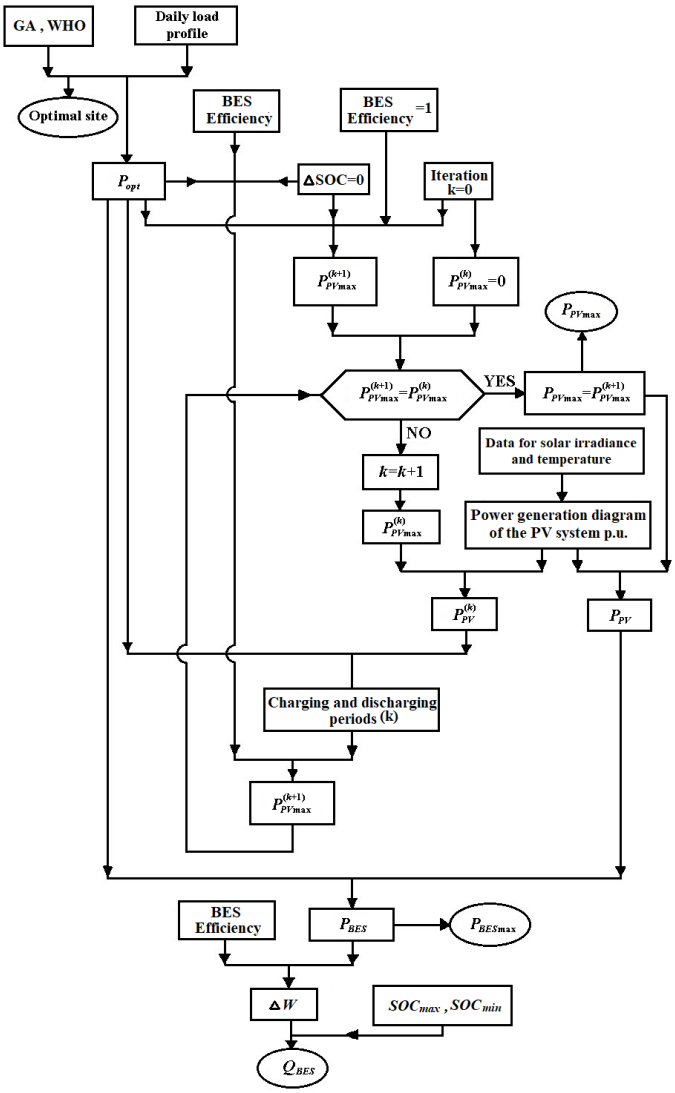

Figure 1. Flowchart of the proposed two-step approach.

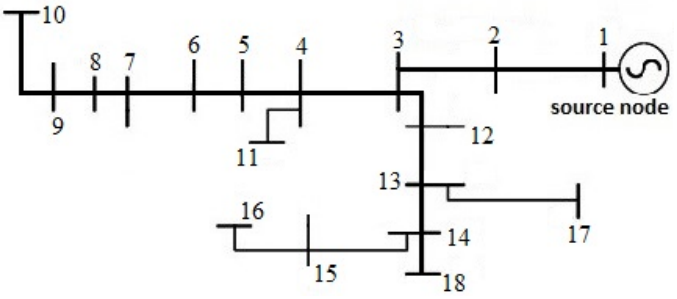

Figure 2. IEEE 18-bus radial DN.

it also represents a suitable test network for smaller distribution systems with fewer nodes.

The overhead DN is used, with the electric parameters $r = 0.4158\,\Omega/\text{km}$ and $x = 0.3807\,\Omega/\text{km}$, and the nominal voltage $U_n = 10\,\text{kV}$. The distance between two adjacent nodes (length of each branch) in the DN is $l = 0.5\,\text{km}$.

The combined type of load is used as the load of

the DN, including 60% resistive (constant impedance load type) and 40% industrial load (constant power load type) on nominal voltage. Three different load diagrams of the DN are used, whose average hourly load powers on 10 kV are shown in Table 1. The first two load diagrams are the cases of high and low matching between the PV power generation and the DN load, while the third one is the realistic DN load diagram.

Table 1. Average hourly load powers of the DN on 10 kV voltage for three different load diagrams.

Hour	P_{LnI} [MW]	P_{LnII} [MW]	P_{LnIII} [MW]
1	1.450	4.500	1.695
2	1.675	4.275	1.375
3	1.900	4.090	1.240
4	2.125	3.640	1.195
5	2.350	3.250	1.330
6	2.575	2.800	1.510
7	2.800	2.575	1.870
8	3.250	2.350	2.220
9	3.640	2.125	2.615
10	4.090	1.900	3.020
11	4.275	1.675	3.480
12	4.500	1.450	3.760
13	4.500	1.450	4.000
14	4.275	1.675	3.500
15	4.090	1.900	3.100
16	3.640	2.125	2.800
17	3.250	2.350	2.490
18	2.800	2.575	2.805
19	2.575	2.800	3.305
20	2.350	3.250	3.800
21	2.125	3.640	3.440
22	1.900	4.090	3.010
23	1.675	4.275	2.310
24	1.450	4.500	1.950

It is important to notice that maximum and average load power for the first two load diagrams is the same $P_{L\,\max,\mathrm{II}} = 4.5\,\mathrm{MW}$ and $P_{L\mathrm{avr,II}} = 2.886\,\mathrm{MW}$, because they have the same hourly powers, which are differently distributed in time. The values of the maximum and average load power for the third load diagram are $P_{L\,\max,\mathrm{III}} = 4.0\,\mathrm{MW}$ and $P_{L\mathrm{avr,III}} = 2.576\,\mathrm{MW}$. Each node in the DN has the same load with the constant power factor, which value for the resistive load is 1 and for industrial load is 0.93.

It is important to emphasize that the used referent voltage is equal to the nominal voltage $U_{\mathrm{ref}} = 10\,\mathrm{kV}$, while the maximum and the minimum allowed values of voltage in the DN are $U_{\max} = 1.1U_n$ and $U_{\min} = 0.9U_n$. The maximum allowed current in the DN is $I_{\max} = 269\,\mathrm{A}$, considering that its branches are made of 70/12 mm^2 Al/Fe conductor.

The average hourly values of the total and diffuse component of the solar irradiance on the horizontal surface and the ambient temperature, for each month are taken from the PVGIS-SARAH3 database for the location of the DN ($L = 43.32°\,\mathrm{N}$ and $\lambda = 21.85°\,\mathrm{E}$). The used value for the reflection coefficient is $\rho = 0.2$, while NOCT is equal to 45°C.

Based on the mentioned values for the solar irradiance and the ambient temperature and using the proposed approach the optimal tilt angle of the PV panels for maximizing the energy generation of the PV system is determined and its value is $\Sigma_{\mathrm{op}} = 32.1°$. Using the optimal value for the tilt angle, the power generation diagram of the PV system, expressed per unit, is obtained for each month and shown in Figure 3.

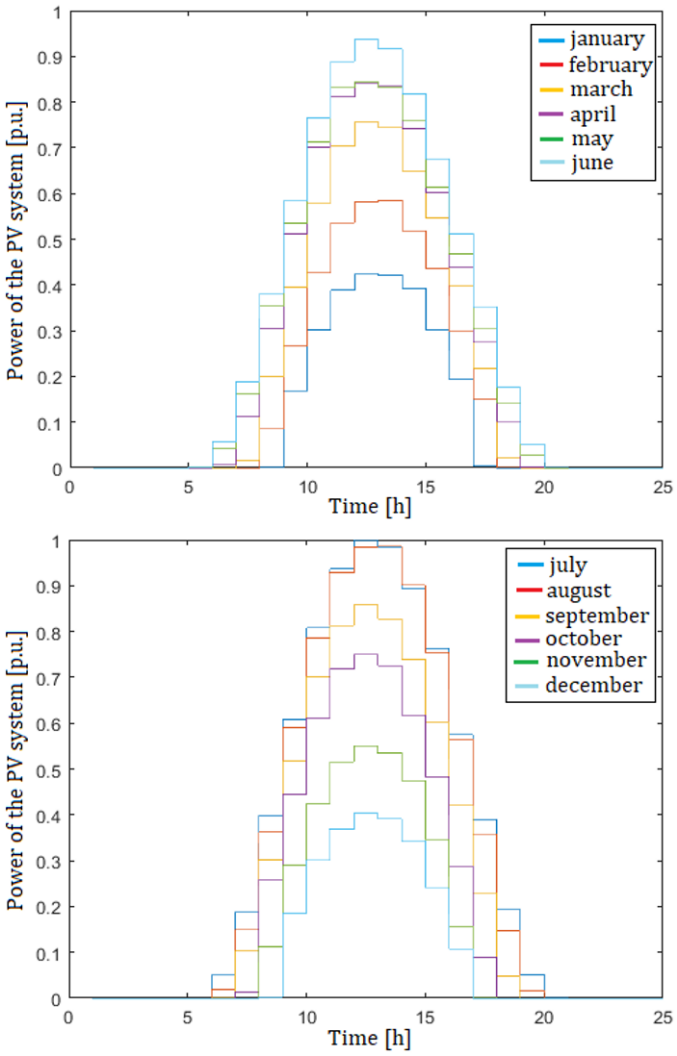

Figure 3. Power generation diagram of the PV system expressed per unit, for the first half of the year (Up) and second half of the year (Down).

Table 2. Voltage quality index of the DN and the optimal location of the PV-BES system in the DN for three different load diagrams

	I load diagram	II load diagram	III load diagram
without PV-BES system	715.408	715.408	566.044
with PV-BES system	18.023	18.023	14.293
	(18.005)	(18.005)	(14.253)
$loc_{\textbf{PV-BES}}$	3	3	3
	(3)	(3)	(3)

From Figure 3, it can be seen that the power generation of the PV system is higher in the summer, when the solar irradiance is greater, than in the winter months, when the solar irradiance has lower values. Also, Figure 3 shows that the power generation of the PV system is highest at noon and does not exist during the night hours. Taking into account (23), the base power for the PV system generation diagram shown in Figure 3 is the maximum power of the PV system over the one-year observation period. This power is not known in advance, but is determined after the optimal sizing of the PV-BES system as the required maximum power of the PV system.

In the implementation of GA 10% of the fittest individuals are allowed to enter the genetic pool, while the probability for mutation is 20%. The WHO is implemented with the values of the coefficients $A_{\max} = 1.2$ and $A_{\min} = 0.6$ using 10 groups of wild horses and the 30% probability of mating. The solution to the optimization problem of determining the optimal location and powers of the PV-BES system is obtained after 50 iterations using the population of 150 individuals. The values of the mentioned control parameters in GA and WHO are obtained from test simulation results, based on which the optimal parameter values are determined. Table 2 presents the values of the voltage quality index in the DN before and after connecting the PV-BES system, as well as the optimal location of the PV-BES system in the DN (i.e., the node index at which it should be connected) for all three load diagrams. It is important to note that the values in brackets are obtained using WHO, while the values without brackets are determined using GA.

Table 2 shows that for all three load diagrams the voltage quality index of the DN is significantly improved after connecting the PV-BES system. The optimal location for connecting the PV-BES system is node 3 of the DN, considering all three load diagrams and both optimization methods. The main reason for this is that from node 3 two main branches of the DN emerged and their load powers have the minimum impact on the DN voltage profile if supplied from node 3. Also, Table 2 shows that voltage quality index of the DN is the same for the first two load diagrams and somewhat lower for the third one, before and after connecting the PV-BES system. This is the direct result of the load powers from the Table 1, which are the same but differently distributed in time for the first and second, and somewhat lower for the third load diagram. In Table 3 are the optimal average hourly powers of the PV-BES.

Table 3. Optimal average hourly powers of the PV-BES system for three different load diagrams.

Hour	I load diagram [MW]	II load diagram [MW]	III load diagram [MW]
1	2.398 (2.386)	7.443 (7.405)	2.760 (2.785)
2	2.770 (2.756)	7.071 (7.034)	2.239 (2.259)
3	3.142 (3.126)	6.765 (6.730)	2.019 (2.037)
4	3.515 (3.497)	6.020 (5.989)	1.946 (1.963)
5	3.887 (3.867)	5.375 (5.348)	2.166 (2.185)
6	4.259 (4.237)	4.631 (4.607)	2.459 (2.481)
7	4.631 (4.607)	4.259 (4.237)	3.045 (3.072)
8	5.375 (5.348)	3.887 (3.867)	3.615 (3.647)
9	6.020 (5.989)	3.515 (3.497)	4.258 (4.296)
10	6.765 (6.730)	3.142 (3.126)	4.918 (4.961)
11	7.071 (7.034)	2.770 (2.756)	5.667 (5.717)
12	7.443 (7.405)	2.398 (2.386)	6.123 (6.177)
13	7.443 (7.405)	2.398 (2.386)	6.514 (6.571)
14	7.071 (7.034)	2.770 (2.756)	5.700 (5.750)
15	6.765 (6.730)	3.142 (3.126)	5.048 (5.093)
16	6.020 (5.989)	3.515 (3.497)	4.560 (4.600)
17	5.375 (5.348)	3.887 (3.867)	4.055 (4.091)
18	4.631 (4.607)	4.259 (4.237)	4.568 (4.608)
19	4.259 (4.237)	4.631 (4.607)	5.382 (5.430)
20	3.887 (3.867)	5.375 (5.348)	6.188 (6.234)
21	3.515 (3.497)	6.020 (5.989)	5.602 (5.651)
22	3.142 (3.126)	6.765 (6.730)	4.902 (4.945)
23	2.770 (2.756)	7.071 (7.034)	3.762 (3.795)
24	2.398 (2.386)	7.443 (7.405)	3.176 (3.203)

Comparing the values with and without brackets in Tables 2 and 3, it can be observed that the results obtained using WHO and GA are practically the same, with negligible differences, although the WHO performs slightly better. The main reason for this lies in the optimization problem itself, which is not very demanding, as it involves the connection of

only one PV-BES system and the minimization of a single-parameter objective function. The second reason is that the results presented in Tables 2 and 3 represent the best outcomes obtained from 20 independent runs of both GA and WHO, using a sufficient number of individuals in the optimization process. Considering that the load power of the DN exhibits the same profile during the first and second 12-hour periods of the day in the first two load diagrams, the optimal power of the PV-BES system follows the same pattern, as shown in Table 3.

Figure 4 shows the voltage in the DN nodes and the currents in the DN branches, before and after the connection of the PV-BES system in the hour of the maximum load. Figure 4 is created using the optimal powers of the PV-BES system from Table 3. Specifically, the optimal powers obtained by the WHO are used, but the same figures with negligible differences would be created using the powers generated by the GA, considering the high level of similarity between the optimal powers obtained by the WHO and GA, shown in Table 3. This also applies to other following results. It is important to emphasize that the index of the DN branch is the same as the index of the node at the end of that branch.

Figure 4 shows that the voltage profile and the currents in the DN branches are the same for the first two load diagrams, which is expected considering the values of the load powers and the optimal powers of the PV-BES system. Taking into account that the load power is somewhat lower in the third load diagram, currents in the DN branches and voltage deviations from the reference value in the DN nodes, are also lower comparing to the first two load diagrams, before and after connecting the PV-BES system (Figure 4).

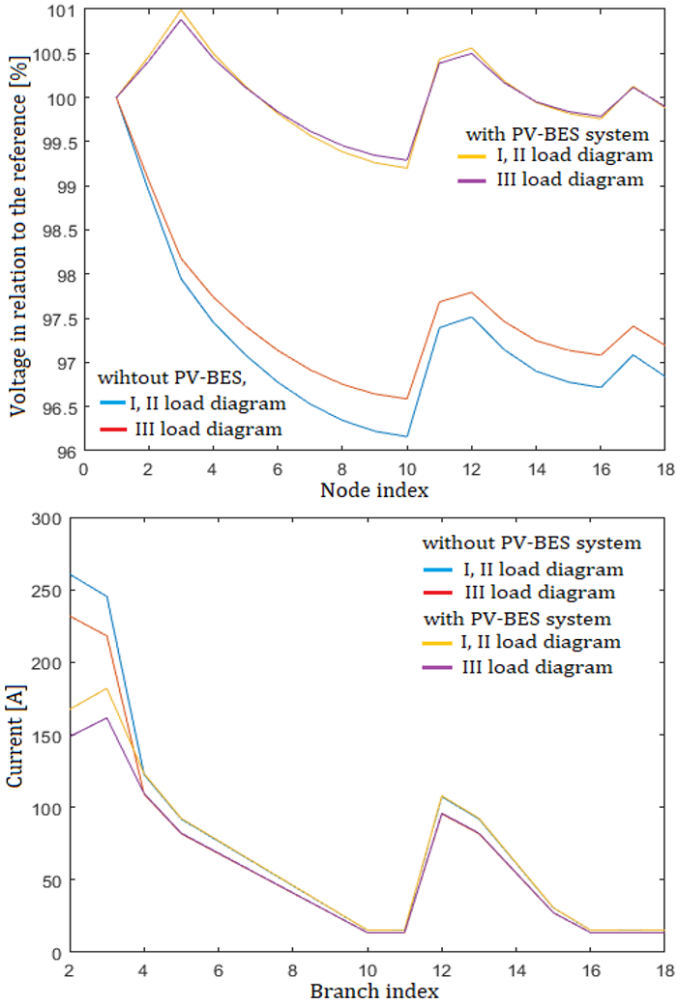

Figure 4. Voltage of the DN nodes (Up) and currents in DN branches (Down) with and without the PV-BES system in the hour of the highest load.

Table 4. Optimal sizing parameters of the PV-BES system for different observation periods for all three load diagrams.

Period	I load diagram			II load diagram			III load diagram		
	P_PV max [MW]	P_BES max [MW]	Q_BES [MWh]	P_PV max [MW]	P_BES max [MW]	Q_BES [MWh]	P_PV max [MW]	P_BES max [MW]	Q_BES [MWh]
Jan.	20.845	13.440	94.303	22.022	19.635	143.154	18.779	12.601	92.366
Feb.	19.000	11.595	82.519	20.119	17.733	132.785	17.129	10.868	82.271
Mar.	18.130	10.725	77.343	19.250	16.863	129.749	16.377	10.198	79.122
Apr.	16.681	9.276	70.725	17.734	15.348	123.858	15.087	8.909	74.111
May.	15.765	8.506	66.689	16.760	14.374	119.567	14.258	8.337	70.460
Jun.	15.861	8.457	64.907	16.863	14.477	117.672	14.346	8.168	68.848
Jul.	15.771	8.366	65.590	16.767	14.381	118.398	14.264	8.086	69.466
Aug.	16.224	8.819	69.053	17.248	14.862	122.080	14.674	8.474	72.598
Sep.	17.422	10.017	73.989	18.496	16.110	126.104	15.735	9.557	76.022
Oct.	18.883	11.478	82.073	20.012	17.626	133.049	17.053	10.875	83.197
Nov.	20.535	13.130	88.243	21.710	19.324	137.396	18.500	12.322	86.900
Dec.	22.063	14.658	94.632	23.304	20.918	143.348	19.873	13.694	92.531
Year	23.445	16.040	378.270	24.825	22.439	443.528	21.159	14.981	348.094

Table 5. Optimal sizing parameters of the PV-BES system for different efficiencies of the BES unit for all three load diagrams

Load Diagram	$\eta = 1.0$			$\eta = 0.95$			$\eta = 0.85$			$\eta = 0.8$		
	P_PV max [MW]	P_BES max [MW]	Q_BES [MWh]	P_PV max [MW]	P_BES max [MW]	Q_BES [MWh]	P_PV max [MW]	P_BES max [MW]	Q_BES [MWh]	P_PV max [MW]	P_BES max [MW]	Q_BES [MWh]
I load diagram	21.294	13.889	360.100	22.294	14.888	368.590	24.787	17.382	389.787	26.366	18.961	402.793
II load diagram	21.294	18.908	406.582	22.927	20.541	424.004	27.053	24.667	465.637	29.694	27.308	490.774
III load diagram	18.973	12.796	329.344	19.982	13.806	337.981	22.520	16.343	359.541	24.132	17.956	372.823

From Figure 4 (Up) it can be seen that the voltage profile of the DN is improved by connecting the PV-BES system, reducing the deviation of the voltage in relation to the reference value under 1% for all DN nodes. This is achieved by reducing (Figure 4 (Down)) and changing the direction of the current in the supply node, shown in Figure 4 (Up), as the increase of the voltage in the first three nodes after connecting the PV-BES system. This means that PV-BES system not only provides the power needed for the load in the DN but also injects power into the supply node to bring the voltage in the DN nodes closer to the referent value. Figure 4 confirms that the voltage and the current in the DN are within their allowed values. The maximum value and the maximum deviation of the voltage from the referent value after connecting the PV-BES system is in the node in which that system is connected, due to its power injection into the DN.

In Table 4, the optimal values of the sizing parameters of the PV-BES system are presented, including the maximum power of the PV system, the maximum power of the BES unit, and the energy capacity of the BES unit, for the first, second, and third load diagrams, respectively. The values in Table 4 are obtained using different observation periods, at the end of which the state of charge of the BES unit must be the same as at the beginning.Specifically, the results in the mentioned Tables are generated using the values of the minimum and maximum allowed state of charge of the BES unit $SOC_{\min} = 0.15$ and $SOC_{\max} = 0.85$ and the efficiency of the charging and discharging processes $\eta = 0.9$.

From Table 4 it can be seen that the sizing parameters of the PV-BES system have higher value in the months with low solar irradiance, as a result of the short period of sunlight during the day. In contrary, in the high solar irradiance months the duration of daylight is longer and thus the needed energy for power injection of the PV-BES system can be produced by the PV system with lower maximum power. The lower maximum power of the PV system produces lower charging rates of the BES unit reducing the needed maximum power of the BES unit for most load diagrams. Also, longer daylight shortens the period in which the optimal powers of the PV-BES system are generated from the BES unit resulting in lower energy capacity of the BES unit and vice versa. Table 4 also show that the highest values of the sizing parameters of the PV-BES system are in the case of the one year observation period. The explanation for this can be found in the fact that in one year period besides the daily variation of the solar irradiance dominant in the observation period of one month, the monthly variation of the solar irradiance is also present, charging the BES unit in high solar irradiance months and discharging it in the low solar irradiance months. This significantly increases the energy exchange between the PV system and the BES unit resulting in much greater energy capacity of the BES unit. Impact of the longer observation period on the maximum powers of the PV system and BES unit is not that high considering that the average load power has not changed.

Table 5 contains the values of the optimal sizing parameters of the PV-BES system for different efficiencies of the BES unit (1, 0.95, 0.85 and 0.8). The allowed state of charge levels are the same as in Table 4.

Using the values from Tables 4 and 5, it can be observed that the maximum power of the PV system predominantly depends on the average load power, which is proportional to the amount of energy that needs to be injected into the DN. The maximum power of the PV system for the third load diagram is approximately 10% lower compared to the first two load diagrams, consistent with their lower average load powers. Beside this, the energy exchange with the BES unit and its efficiency also have certain impact on the PV system maximum power because they define the energy losses that need to be covered by the PV system generation (maximum power of the PV system is highest for the second load diagram). On the other hand, Tables 4 and 5 show that the highest maximum power and energy capacity of the BES unit is obtained for the second load diagram where the matching between the PV system power generation and the load power is the lowest. It is important to point out that the values of the maximum powers of the PV system from Tables 4 and 5 are generated after 2 iterations of the

proposed iterative method for the observation period of one month, and after 3 iterations for the observation period of one year.

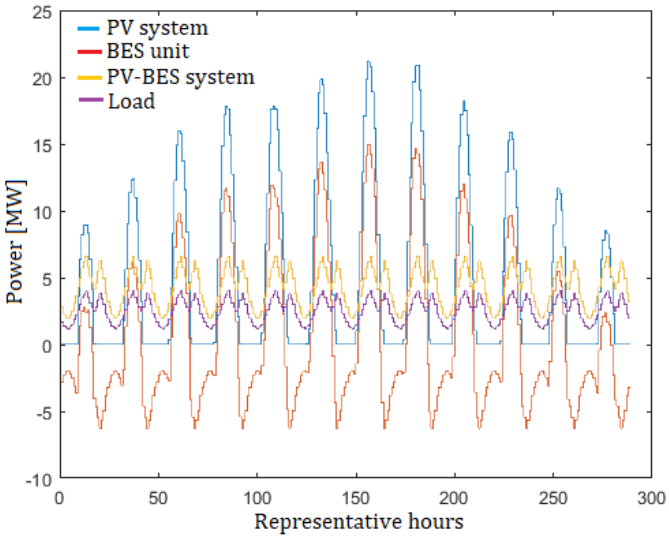

Figure 5. Optimal powers of the PV system, BES unit and PV-BES system, in the one year observation period (288 representative hours) for the third load diagram.

Figure 5 represents the optimal powers of the PV system, BES unit and PV-BES system, in the one year observation period for the third load diagram, as the most realistic one. Considering that the average hourly values of the solar irradiance for each month in the year are used, the observation period of one month is composed of 24 representative hours, while the observation period of one year is composed of 288 representative hours, as shown on Figures 5 and 7.

The mentioned optimal powers of the PV system, BES unit and the PV-BES system in the month of July (month with the highest PV generation) for the first, second and the third load diagram, are shown in Figure 6.

In Figures 5 and 6, it is shown that during periods of high solar irradiance, the optimal power of the PV-BES system is generated by the PV system, while the BES unit is charging ($P_{BES} > 0$). During periods of low solar irradiance, the required power is supplied by discharging the BES unit ($P_{BES} < 0$). Also, these figs. show that the shape of the power of the PV system is the same as in its power generation diagrams from Figure 3, while the optimal power of the PV-BES system follows the shape of the load power in the DN, but has the greater values. As mentioned earlier the optimal power of the PV-BES system must be greater than the load power to achieve the negative voltage drop in certain DN branches and maintain the voltage

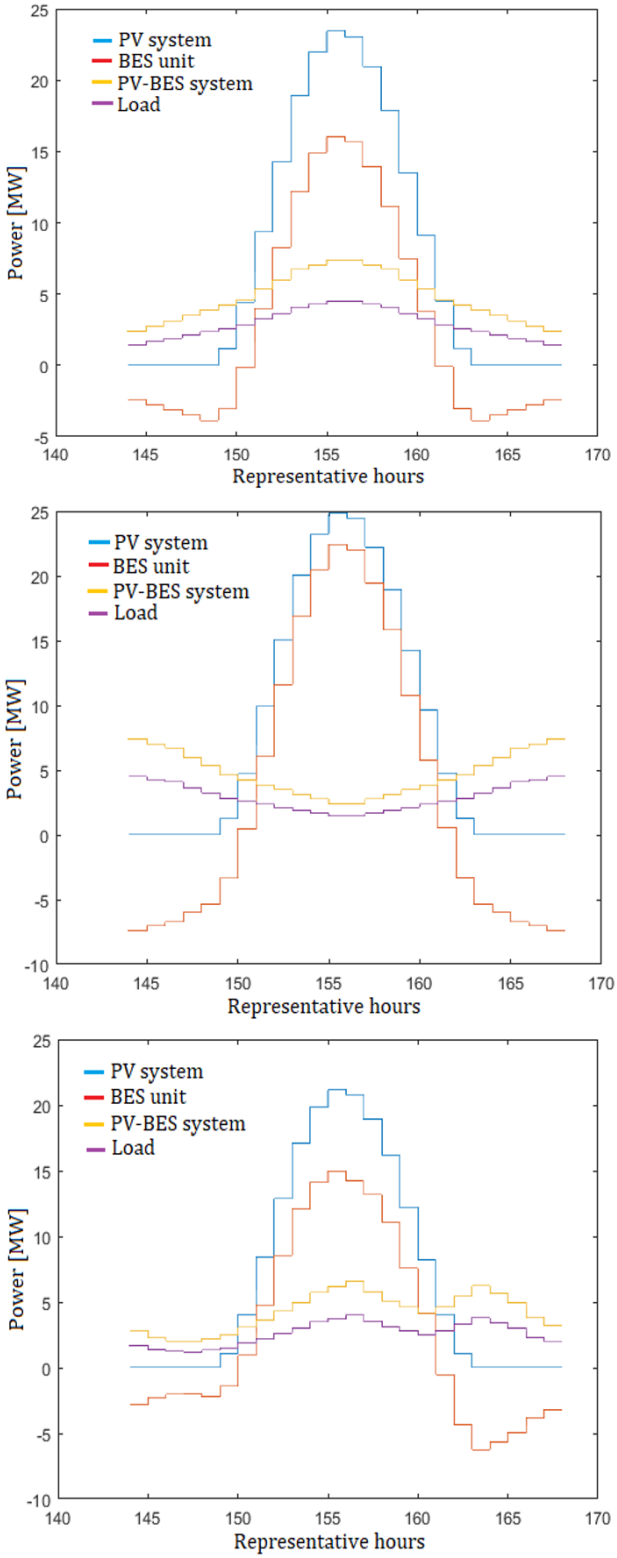

Figure 6. Optimal powers of the PV system, BES unit and the PV-BES system, in July (145-168 representative hour) for the first (Up), second (Middle) and the third load diagram (Down).

in the DN nodes closer to the referent value.

Figure 7 shows the state of charge of the BES unit for all three load diagrams in the one year observation period.

From Figure 7, it can be seen that the state of charge of the BES unit is between its minimum and maximum allowed values (0.15 and 0.85) and is the same at the beginning and at the end of the observation period.

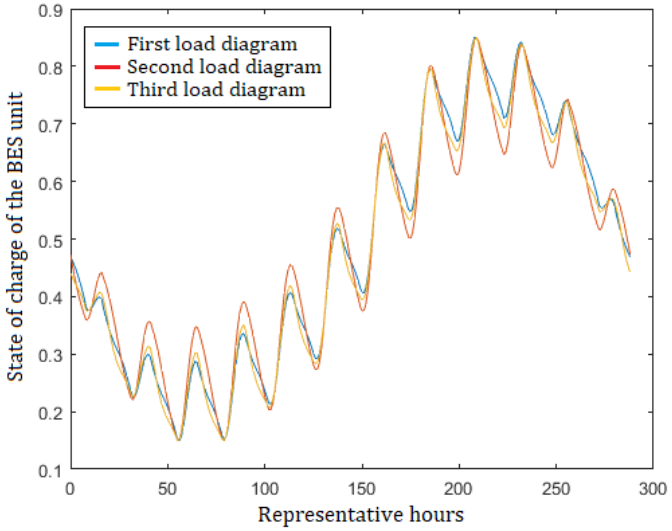

Figure 7. State of charge of the PV-BES system in the one year observation period (288 representative hours) for all three load diagrams.

Also, Figure 7 shows that the state of charge of the BES unit changes its value on daily basis due to the intermittent character of the solar irradiance during the day and on monthly basis due to the monthly variation of the solar irradiance during the year (in the first three months the state of charge is decreasing, the next six months is increasing and again decreasing in the last three months). The highest daily variations of the state of charge of the BES unit are obtained for the second load diagram when the exchange of the energy between the PV system and the BES unit is highest due to the low matching between the load and the PV generation. For the same reason the daily variations of the state of charge are the lowest for the first load diagram, as can be seen from Figure 7.

To demonstrate the performance of the employed meta-heuristic optimization methods, Figure 8 and Table 6 are prepared based on the values of the criterion function obtained during the determination of the optimal location and optimal powers of the PV-BES system for the third load diagram, which is considered the most representative one. Specifically, Figure 8 shows the convergence of the criterion function throughout the iterations, obtained using WHO and GA for five different runs of optimization.

Although the criterion function converges (the optimal solution is found) after similar number of iterations for

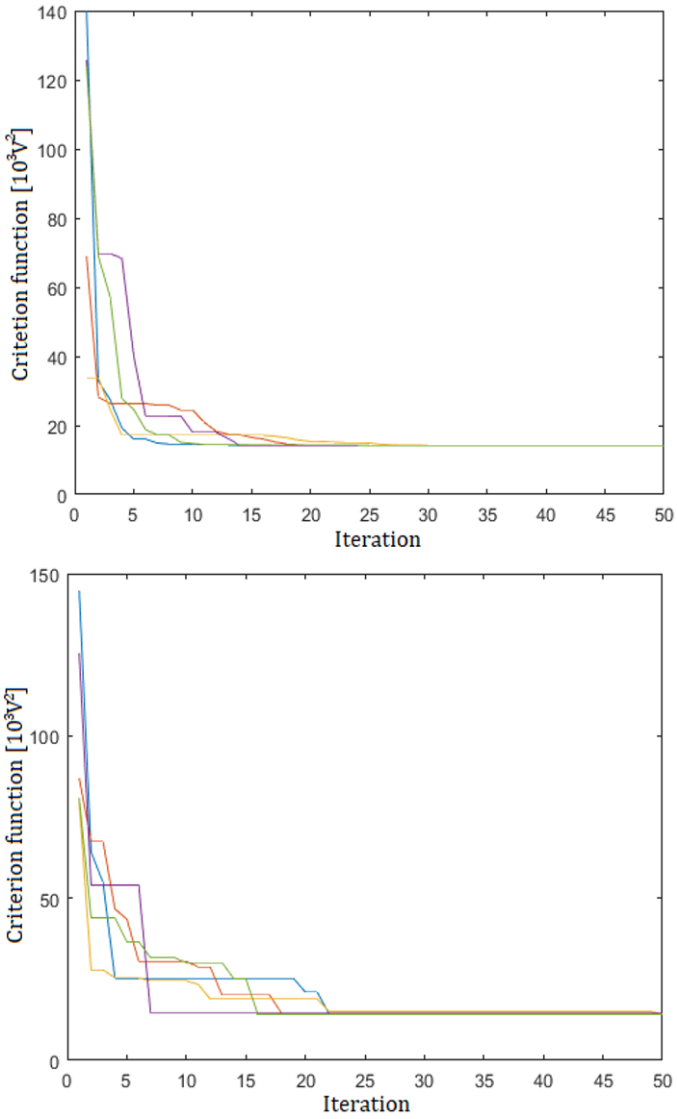

Figure 8. Convergence of the criterion function throughout the iterations obtained using WHO (Up) and GA (Down) for five different runs.

both optimization methods, Figure 8 shows that the convergence is more gradually in the case of WHO. It is important to emphasize that the simulations used for generating results were performed on the laptop with the following hardware characteristics: Intel i5 CPU 2.5 GHz and 6 GB RAM. Average computation time for finding the solution to the optimization problem in one attempt (after 50 iterations using the population of 150 individuals) on the mentioned hardware is 16.15 seconds in the case of GA and 10.37 seconds in the case of WHO. In Table 6, the values of the statistical indicators including minimal value, maximal value, mean value and the standard deviation are shown for both optimization methods generated after 50 runs.

As can be seen from Table 6, WHO again demonstrates better performance compared to GA, considering the

Table 6. Values of the statistical indicators obtained using both optimization methods after 50 runs.

Optimization method	Min. value $[10^3V^2]$	Max. value $[10^3V^2]$	Mean value $[10^3V^2]$	$\sigma[V^2]$
GA	14.253292	14.878940	14.323420	149.7667
WHO	14.253122	14.253318	14.253180	0.050544

lower values of all statistical indicators obtained for this optimization method. Table 6 also shows that although both optimization methods have achieved very similar minimum values of the criterion function, WHO has a greater probability of reaching this value or a value very close to it, as indicated by the significantly lower standard deviation.

6 Conclusion

In this paper the two-step approach for improving the voltage profile of the DN through the optimal integration of the PV-BES system is presented. The results show that the voltage profile of the DN can be significantly improved by the optimal siting and sizing the PV-BES system, reducing the voltage deviation from the referent value under 1%. The meta-heuristic optimization methods of WHO and GA prove to be vary suitable for finding the optimal location and optimal powers of the PV-BES system, determining it in around 25 iterations, whereby the WHO showed better performances considering statistical parameters. The proposed iterative method for optimal sizing the PV-BES system show high efficiency, finding the maximum power of the PV system under 4 iterations.

The obtained results confirm that the optimal power injection of the PV-BES system depends on and follows the shape of the load power, with the value that is around 60% higher than the load. The maximum power of the PV system dominantly depends on the average load power and is around 7 to 9 times higher depending on the efficiency of the BES unit. The results show that the maximum power and the energy capacity of the BES unit increase their values if the matching between the PV generation and the load in the DN decreases. Also, the values of the sizing parameters of the PV-BES system are higher in the case of lower efficiency of the charging and discharging process of the BES unit. Specifically results show, that the energy capacity of the BES unit is inversely proportional to the efficiency of the BES unit, while the maximum power of the BES unit is inversely proportional to the squared value of the efficiency of the BES unit.

Data Availability Statement

Data will be made available on request.

Funding

This work was supported by the Ministry of Science, Technological Development and Innovation of the Republic of Serbia under Grant 451-03-34/2026-03/200102.

Conflicts of Interest

The authors declare no conflicts of interest.

AI Use Statement

The authors declare that no generative AI was used in the preparation of this manuscript.

Ethical Approval and Consent to Participate

Not applicable.

References

[1] Pokhrel, B., Shrestha, A., Phuyal, S., & Jha, S. (2021). Voltage profile improvement of distribution system via integration of distributed resources. *Journal of Renewable Energy, Electrical, and Computer Engineering, 1*(1), 33-41. [CrossRef]

[2] Mijailović, V. (2011). *Distribuirani izvori energije*. Beograd: Akademska misao.

[3] Elattar, E., & Elsayed, S. (2020). Optimal location and sizing of distributed generators based on renewable energy sources using modified moth flame optimization technique. *IEEE Access, 8*, 109625-109638. [CrossRef]

[4] Lamsal, D., Mishra, A., & Gautam, P. (2016, June 1-3). Optimal location and sizing of distributed generation: B-coefficient matrix approach. In *12th IEEE International Conference on Control and Automation (ICCA)* (pp. 810-815). Kathmandu, Nepal. [CrossRef]

[5] Das, C., Bass, O., Mahmoud, T., Kothapalli, G., Masoum, M., & Mousavi, N. (2019). An optimal allocation and sizing strategy of distributed energy storage systems to improve performance of distribution networks. *Journal of Energy Storage, 26*, 100847. [CrossRef]

[6] Chiang, M., Huang, S., Hsiao, T., Zhan, T., & Hou, J. (2022). Optimal sizing and location of photovoltaic generation and energy storage systems in an unbalanced distribution system. *Energies, 15*(18), 6682. [CrossRef]

[7] Singh, A., Shrestha, A., Phuyal, S., Adhikari, B., & Papadakis, A. (2018). Particle swarm optimization

approach for distributed generation allocation planning for voltage profile improvement. In *11th International Conference on Deregulated Engineering Market Issues in South Eastern Europe, Nicosia, Cyprus*.

[8] Radosavljević, J. (2021). Voltage regulation in LV distribution networks with PV generation and battery storage. *Journal of Electrical Engineering, 72*(6), 356-365. [CrossRef]

[9] Bai, W., Zhang, W., Allmendinger, R., Enyekwe, I., & Lee, K. Y. (2024). A comparative study of optimal pv allocation in a distribution network using evolutionary algorithms. *Energies, 17*(2), 511. [CrossRef]

[10] Mossie, M. A., Yetayew, T. T., Bitew, G. T., Yenealem, M. G., & Beza, T. M. (2025). Adaptive genetic algorithm and enhanced particle swarm optimization for static voltage stability enhancement in radial distribution systems with distributed generation integration. *Discover Applied Sciences, 7*(12), 1414. [CrossRef]

[11] Zheng, R., Hussien, A., Jia, H., Abualigah, L., Wang, S., & Wu, D. (2022). An improved wild horse optimizer for solving optimization problems. *Mathematics, 10*(8), 1311. [CrossRef]

[12] Ali, M., Kamel, S., Hassan, M., Tostedo-Veliz, M., & Zawbaa, H. (2022). An improved wild horse optimization algorithm for reliability based optimal DG planning of radial distribution networks. *Energy Reports, 8*, 582-604. [CrossRef]

[13] Radosavljević, J. (2018). *Metaheuristic Optimization in Power Engineering*. London: Institution of Engineering and Technology. [CrossRef]

[14] Adetunji, K., Hofsajer, I., Abu-Mahfouz, A., & Cheng, L. (2020). A review of metaheuristic techniques for optimal integration of electrical units in distribution network. *IEEE Access, 9*, 5046-5068. [CrossRef]

[15] Milovanović, M. J., Radosavljević, J. N., & Perović, B. D. (2025). Taguchi-Based Parameter Tuning of PSO for Optimal Capacitor Placement in Unbalanced Distribution Systems. *ICCK Transactions on Electric Power Networks and Systems, 1*(1), 6-16. [CrossRef]

[16] Krstic, N. N., Tasic, D. S., Klimenta, D. O., & Milovanovic, M. J. (2024). Improving the Operation of a Distribution Network by Optimal Siting and Sizing of Photovoltaic-Battery Energy Storage Systems. *Elektronika ir Elektrotechnika, 30*(5), 70-82. [CrossRef]

[17] Khenissi, I., Guesmi, T., Marouani, I., Alshammari, B. M., Alqunun, K., Albadran, S., ... & Neji, R. (2023). Energy management strategy for optimal sizing and siting of PVDG-BES systems under fixed and intermittent load consumption profile. *Sustainability, 15*(2), 1004. [CrossRef]

[18] Wong, L., Ramachandaramurthy, V., Walker, S., & Ekanayake, J. (2020). Optimal placement and sizing of battery energy storage system considering the duck curve phenomenon. *IEEE Access, 8*, 197236-197248. [CrossRef]

[19] Wong, L. A., Shareef, H., Mohamed, A., & Ibrahim, A. A. (2017). Optimal placement and sizing of energy storage system in distribution network with photovoltaic based distributed generation using improved firefly algorithms. *World Academy of Science, Engineering and Technology, International Journal of Electrical, Computer, Energetic, Electronic and Communication Engineering, 11*(7), 864-872.

[20] Tang, X., Deng, K., Wu, Q., & Feng, Y. (2020). Optimal location and capacity of the distributed energy storage system in a distributed network. *IEEE Access, 8*, 15576-15585. [CrossRef]

[21] Ibrahim, H. O., Moustapha, M. D., Gonda, M., & Issaka, A. M. M. (2026). Multi-objective optimization of the combined sizing and placement of a PV system and an UPQC in an IEEE 69-bus distribution network using genetic algorithm. *International Journal of Energy and Power Engineering, 15*(1), 37-44. [CrossRef]

[22] Ahmed, H. M., Calucag, L. S., Alqahtani, H., Noaman, N. M., Ismail, Z. M., & Alhawi, O. A. (2024, November). Seasonal analysis of PV performance: optimizing fixed panel angles for maximum efficiency. In *2024 IEEE 9th International Conference on Engineering Technologies and Applied Sciences (ICETAS)* (pp. 1-4). IEEE. [CrossRef]

[23] Mansouri, N., Lashab, A., Guerrero, J., & Cherif, A. (2020). Photovoltaic power plants in electrical distribution networks: A review on their impact and solutions. *IET Renewable Power Generation, 14*(12), 2114-2125. [CrossRef]

[24] Mikulović, J., & Đurišić, Z. (2019). *Solarna energetika*. Belgrade: Akademska misao.

[25] Bala, A., Moshood Alao, B., Olamide Oyedun, A., Omotayo Alabi, O., & Adamu, M. (2024). Performance evaluation of a solar photovoltaic (PV) module at different solar irradiance. *International Journal of Engineering & Applied Sciences (IJEAS), 16*(2), 63-75. [CrossRef]

[26] Klimenta, D., Lekic, J., Arsic, S., Tasic, D., Krstic, N., & Radosavljevic, D. (2021). A novel procedure for quick design of off-grid PV water pumping systems for irrigation. *Elektronika Ir Elektrotechnika, 27*(2), 64-77. [CrossRef]

[27] Kamali, G. A., Moradi, I., & Khalili, A. (2006). Estimating solar radiation on tilted surfaces with various orientations: a study case in Karaj (Iran). *Theoretical and applied climatology, 84*(4), 235-241. [CrossRef]

[28] Mikulović, J., Đurišić, Ž., & Kostić, R. (2013). Određivanje optimalnih nagibnih uglova fotonaponskih panela. *Infoteh, Mart*.

[29] Calabrò, E. (2012). The disagreement between anisotropic-isotropic diffuse solar radiation models as a function of solar declination: computing the optimum tilt angle of solar panels in the area of southern-Italy. *Smart Grid and Renewable Energy, 3*(4),

253-259. [CrossRef]

[30] Milovanović, M. J., Dragičević, M. M., Krečković, N. R., & Perović, B. D. (2025). Short-Term Load Forecasting with Taguchi-Optimized Single-Layer Feedforward Neural Networks: A MATLAB GUI. *ICCK Transactions on Electric Power Networks and Systems, 1*(2), 70-81. [CrossRef]

[31] Tuka, B. M., & Ali, E. S. (2026). Optimal allocation and sizing of distributed generation for improvement of distribution feeder loss and voltage profile in the distribution network using genetic algorithm. *Measurement and Control, 59*(2), 217-231. [CrossRef]

[32] Motwakel, A., Alabdulkreem, E., Gaddah, A., Marzouk, R., Salem, N. M., Zamani, A. S., ... & Eldesouki, M. I. (2023). Wild horse optimization with deep learning-driven short-term load forecasting scheme for smart grids. *Sustainability, 15*(2), 1524. [CrossRef]

[33] Seyednouri, S. N., Ebrahimian, H., & Jalili, A. (2015). Power loss reduction and voltage profile improvement by photovoltaic generation. *International Journal of Engineering Trends and Technology (IJETT), 20*(4), 192-196. [CrossRef]

[34] Belsky, A., Glukhanich, D., Sutikno, T., & Jopri, M. H. (2023). Estimation of hourly solar irradiation on tilted surfaces. *Bulletin of Electrical Engineering and Informatics, 12*(6), 3202-3214. [CrossRef]

[35] Azarbakhsh, G., Mahmoudi, A., Kahourzade, S., Yazdani, A., & Mahmud, A. (2025). Optimal sizing of photovoltaic and battery energy storage for residential houses in South Australia by considering vehicle-to-home operation. *IET Renewable Power Generation, 19*(1), 70053. [CrossRef]

[36] Mumtahina, U., Alahakoon, S., & Wolfs, P. (2025). Optimal allocation and sizing of battery energy storage system in distribution network using mountain gazelle optimization algorithm. *Energies, 18*, 379-397. [CrossRef]

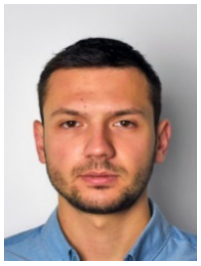

Nikola Krstić was born on 24 February 1995 in Niš. He graduated in 2018 and completed his master's academic studies in 2019 at the Faculty of Electronics in Niš. His main areas of interest include distribution network analysis, power systems optimization using meta-heuristic optimization methods, and photovoltaic systems. He is currently a Ph.D. student and works as an assistant at the Department of Electric Power Engineering at the Faculty of Electronic Engineering in Niš. (Email: nikola.krstic@elfak.ni.ac.rs)

Dragan Tasić was born in Serbia, in 1961. He graduated from the Faculty of Electrical Engineering, University of Belgrade, in 1986. Also, he received his postgraduate M.Sc. in 1991 from the Faculty of Electrical Engineering, University of Belgrade, and Ph.D. in 1997 from Faculty of Electronic Engineering, University of Niš. His main research interests include electrical power cable engineering, renewable energy sources, electric power system modeling and analysis, heat transfer and optimization methods. Currently, he is a Full Professor with the Faculty of Electronic Engineering, University of Niš. (Email: dragan.tasic@elfak.ni.ac.rs)